CONF-760716--2

LA-UR-76-1408

TITLE: COMPRESSION STUDIES OF FORSTERITE (Mg_2SiO_4) AND ENSTATITE ($MgSiO_3$)

AUTHOR(S): Bart W. Olinger

SUBMITTED TO: U. S. - Japan Seminar "High Pressure Research Applications in Geophysics"

By acceptance of this article for publication, the publisher recognizes the Government's (license) rights in any copyright and the Government and its authorized representatives have unrestricted right to reproduce in whole or in part said article under any copyright secured by the publisher.

The Los Alamos Scientific Laboratory requests that the publisher identify this article as work performed under the auspices of the USERDA.

los alamos
scientific laboratory
of the University of California
LOS ALAMOS, NEW MEXICO 87545

An Affirmative Action/Equal Opportunity Employer

NOTICE
This report was prepared as an account of work sponsored by the United States Government. Neither the United States nor the United States Energy Research and Development Administration, nor any of their employees, nor any of their contractors, subcontractors, or their employees, makes any warranty, express or implied, or assumes any legal liability or responsibility for the accuracy, completeness or usefulness of any information, apparatus, product or process disclosed, or represents that its use would not infringe privately owned rights.

Form No. 836
St. No. 2629
1/75

UNITED STATES
ENERGY RESEARCH AND
DEVELOPMENT ADMINISTRATION
CONTRACT W-7405-ENG. 36

MASTER

DISTRIBUTION OF THIS DOCUMENT IS UNLIMITED

COMPRESSION STUDIES OF FORSTERITE (Mg_2SiO_4) AND ENSTATITE ($MgSiO_3$)

Bart Olinger

Los Alamos Scientific Laboratory

Los Alamos, New Mexico

87545

ABSTRACT

From hydrostatic high pressure, x-ray diffraction studies of forsterite, Mg_2SiO_4, and enstatite, $MgSiO_3$, the following zero pressure isothermal bulk moduli and their pressure derivatives were determined

	ρ_o	B_{ot}	B'_{ot}
forsterite	3.234 g/cm^3	120 GPa	5.6
enstatite	3.227 g/cm^3	125 GPa	5 (assumed)

The cell edge (linear) and volume compressions are compared with those calculated from elastic constants [Graham and Barsch, 1969], Frisillo and Barsh, 1972] and with shock compression data [Ahrens, Lower, and Lagus, 1971], [Ahrens and Gaffney, 1971].

Forsterite and enstatite are end members of two important mineral series thought to make up a large portion of the earth's upper mantle. Evidence for this hypothesis can be found in comparisons of seismic data and mass distribution models of the earth with the densities and sound velocities of these minerals under pressure. Recently there have been several determinations of both densities and sound speeds of these minerals under both static and dynamic stress. Kumazawa and Anderson [1969] and Graham and Barsch [1969] measured the elastic constants of forsterite, Mg_2SiO_4, and Ahrens, Lower, and Lagus [1971] determined the dynamic compression of forsterite. Kumazawa [1969] and Frisillo and Barsch [1972] measured the elastic constants of orthopyroxenes, $(Mg_{.85}, Fe_{.15})\ SiO_3$ and $(Mg_{.8}, Fe_{.2})\ SiO_3$ respectively, and Ahrens and Gaffney [1971] determined the dynamic compression of orthopyroxene, $(Mg_{.86}, Fe_{.14})\ SiO_3$. Here are reported some recent measurements of the linear and volume compression of both enstatite and forsterite using a hydrostatic high pressure, x-ray diffraction technique. The linear compressions are compared with the values calculated for forsterite [Graham and Barsch, 1969] and for bronzite [Frisillo and Barsch, 1972] from elastic constant data. The bulk moduli are also compared with those derived from ultrasonic data. The isothermal compression fits are then converted to shock-particle velocities along the Hugoniot and compared with the results of Ahrens, Lower and Lagus [1971] and Ahrens and Gaffney [1971].

The technique used here has been described earlier [Halleck and Olinger, 1974]. Briefly, an annulus of beryllium 2.5 mm in dia., 0.2 mm thick with a 0.2 mm dia hole at its center is pressed between two tungsten carbide Bridgman anvils. The hole is filled with a mixture of powdered

sample and powdered aluminum or NaF (the pressure indicators), and a mixture of 4:1 methanol-ethanol that remains liquid to 10 GPa [Piermarini et al., 1973]. A CuKα x-ray beam is directed through the annulus and the diffraction is recorded on a 114.6 mm dia cylindrical film surrounding the annulus.

The forsterite, Mg_2SiO_4, studied here was a synthesized hot pressed compound. Microprobe analysis indicated good homogenity. There was minor interstitial contamination from carbon, but this did not effect the diffraction patterns of the material. The diffraction pattern of the forsterite at ambient conditions yielded the following orthorhombic cell edge parameters; $\underline{a}$ = 4.7470 ± 0.0018 Å, $\underline{b}$ = 10.1800 ± 0.0035 Å, and $\underline{c}$ = 5.9771 ± 0.0012 Å. The calculated crystal density is 3.234 g/cm^3. The enstatite, $MgSiO_3$, came from the Mt. Egerton meteorite, Australia (an enstatite achondrite). The chemical analysis of the enstatite is given by Reid and Cohen [1967]. The major impurities are Ca (.33 wt%), excess SiO_2 (.33%), Al (.02 wt%) and Mn (.02 wt%). The diffraction pattern of the enstatite at ambient condition yielded the following orthorhombic cell edge parameters; $\underline{a}$ = 8.8189 ± 0.0038 Å, $\underline{b}$ = 18.2205 ± 0.0095 Å, and $\underline{c}$ = 5.1803 ± 0.0028 Å. The calculated crystal density is 3.227 g/cm^3.

The pressures were determined from the diffraction patterns of the NaF or Al mixed with the sample. The two lines read from the NaF were the (200) and (220). The three lines read from the Al were the (111), (220) and (311). The standard patterns for the NaF and Al are given by Swanson and Tatge [1953] (a_o = 4.6342 Å and 4.0494 Å respectively). The relative volumes, V/V_o, of these two materials

are correlated with pressures to 13 GPa (130 kbar) elsewhere [Olinger and Halleck, 1976].

The quality of the forsterite x-ray diffraction patterns was usually good. The d-spacings were determined at high pressures for the following planes: (021), (101), (130), (131), (112), (004), and the (062). The quality of the enstatite diffraction patterns at high pressures was not good, and the d-spacings measured had 2-theta diffraction angles of less than 40° (up to 65° for forsterite). The lines measured at high pressures were for the following planes: (211), (240), (160), (311) and (022). The problems for enstatite were compounded by no agreement among the crystallographic literature for the indexing of higher angle lines and the necessary use of an overground sample which could not be readily replaced (too fine ground powder causes poor coherent diffraction.)

In Tables 1 and 2 the data are listed in the form of the relative volumes of the pressure indicators, the correlated pressures, the relative cell edges, the relative volumes and the shock-particle velocity analogues, U_{st} and U_{pt} [Olinger and Halleck, 1976]. In Figs. 1 and 3, the relative volumes calculated from elastic constants of forsterite [Graham and Barsch, 1969], and of bronzite [Frisillo and Barsch, 1972]. In Figs. 2 and 4 the U_{st}, U_{pt} values are plotted along with the loci of the shock-particle velocities, U_s-U_p, calculated from the same elastic constants. Also plotted in Figs. 2 and 4 are the U_s-U_p data of Ahrens, Lower and Lagus [1971] and Ahrens and Gaffney [1971].

It is obvious from Fig. 1 that the relative volumes, $V(P)/V_o$, for forsterite calculated from the elastic constants [Graham and Barsch, 1969] are in excellent agreement with the present x-ray data.

However, the x-ray data shows the b axis or cell edge to be less compressible than that calculated from the elastic constants, and the a axis to be more compressible.

In Fig. 2 the x-ray data are plotted in terms of U_{st}, $(PV_o/(1-V/V_o))^{1/2}$, and U_{pt}, $(PV_o/(1-V/V_o))^{1/2}$. V is the specific volume (see Olinger and Halleck, [1975]). The intercept of a linear fit to U_{st}, U_{pt} data is the zero-pressure bulk sound speed of the material. The slope of the linear fit is related to the pressure derivative of the zero pressure isothermal bulk modulus as given by the following expression

$$s_t = (B'_{ot} + 1)/4. \quad (1)$$

The linear fit to the present forsterite data is

$$U_{st} = 6.09 + 1.65\ U_{pt}. \quad (2)$$

From this fit the isothermal zero pressure bulk modulus is calculated to be 120 GPa (1.20 Mbar). This value compares well with the values calculated from the ultrasonic data, 128.0 GPa [Graham and Barsch, 1969] and 127.5 GPa [Kumazawa and Anderson, 1969]. The pressure derivative of the modulus determined from the slope is 5.6, and this also compares well with the values determined from ultrasonic data, 5.0 and 5.4 respectively.

The linear fit to the x-ray data is shown in Fig. 2, along with the Hugoniots derived from the ultrasonic data. In the same figure are the low pressure shock compression data of Ahrens, Lower and Lagus [1971]. As is shown, there is poor agreement between the the calculated Hugoniots derived from the x-ray and ultrasonic data, and the shock data. The reason for the disagreement seems to be caused by the porosity of the samples of Ahrens, Lower and Lagus [1971]

which was not less than 4% for the data in Fig. 2.

In Fig. 3 the relative cell edges and volumes of bronzite, $(Mg_{.8}Fe_{.2})\ SiO_3$, calculated from ultrasonic data [Frisillo and Barsch, 1972] are compared with the present x-ray data for enstatite, $MgSiO_3$. Despite the scatter in the x-ray data, two conclusions can be reached. The first is that the a axis in enstatite is not as compressible as that determined for bronzite. It is of interest to note that with increasing FeO content, the a axis expands more than the other cell edges. This is possibly a direction of weak bonding and repulsion. Because of the less compressible a axis, the volume of enstatite is found to be less compressible than that of bronzite.

In Fig. 4 the x-ray data are plotted in terms of U_{st} and U_{pt}. The scatter is great enough to prohibit any reasonable linear fit directly to the data. Instead, a value for the slope is assumed, 1.5 ($B'_{ot} = 5$), and an intercept is calculated for each datum. The average of these is 6.22 ± 0.19 km/s. Thus the linear fit estimated for the x-ray data is

$$U_{st} = 6.22 + 1.5\ U_p. \qquad (3)$$

This implies a bulk modulus of 125 ± 8 GPa assuming B'_{ot} equals 5. For bronzite, $(Mg_{.8}Fe_{.2})\ SiO_3$, Frisillo and Barsch [1972] measured a bulk modulus of 98.8 GPa and a derivative of 9.5 (see Fig. 4). (From our data, $B_o = 115 \pm 8$ GPa if $B'_o = 9.5$) The large pressure derivative of the bulk modulus is not substantiated by the Hugoniot data of Ahrens and Gaffney [1969]. They studied nearly the same mineral as Frisillo and Barsch [1972] and for that study the samples had no porosity. The low pressure data (below 30 GPa) is plotted

also in Fig. 4. An equilibrium Hugoniot can be calculated by using the adiabatic bulk sound speed of Frisillo and Barsch [1972] as the intercept and averaging the slope through the Hugoniot data. The Hugoniot is

$$U_s = 5.55 + 1.10\ U_p. \tag{4}$$

The pressure derivative for the zero pressure bulk modulus is 3.4 for this fit. This result is also supported by the shock compression of a bronzitite rock (Stillwater complex, Montana) [McQueen, Marsh, and Fritz 1967]. The composition of the bronzitite was 94% bronzite, $(Mg_{.9}Fe_{.1})\ SiO_3$. The linear fit to the data before the onset of a 35 GPa phase transition is

$$U_s = 6.10 + 1.01\ U_p. \tag{5}$$

The pressure derivative of the bulk modulus in this case is 3.04. Thus, I conclude that the estimate of the slope in Eq. (3) is reasonable.

ACKNOWLEDGMENTS

This work was supported by the U. S. Energy Research and Development Administration. This paper was presented as the U. S.-Japan Seminar "High Pressure Research Application in Geophysics" July 6-9, 1976, Honolulu, Hawaii, which was sponsored by the National Science Foundation.

TABLE 2. THE COMPRESSION OF ENSTATITE

V/V_o *	P +	a/a_o *	b/b_o *	c/c_o *	V/V_o *	U_{st} +	U_{pt} +
N: NaF A: Al	(GPa)	enstatite					
.9749 (08) A	2.03 (.06)	.9949 (03)	.9940 (03)	.9959 (02)	.9848 (04)	6.44 (.13)	0.098 (.002)
.9658 (05) A	2.85 (.04)	.9924 (15)	.9931 (16)	.9936 (14)	.9752 (26)	6.52 (.41)	0.136 (.008)
.9586 (07) A	3.52 (.06)	.9915 (09)	.9911 (09)	.9916 (08)	.9744 (15)	6.53 (.21)	0.167 (.005)
.9362 (15) N	3.65 (.11)	.9895 (13)	.9914 (07)	.9916 (30)	.9727 (33)	6.44 (.39)	0.176 (.011)
.9495 (04) A	4.41 (.04)	.9893 (04)	.9902 (04)	.9896 (04)	.9694 (07)	6.68 (.08)	0.205 (.002)
.9240 (05) N	4.51 (.03)	.9827 (19)	.9920 (20)	.9897 (18)	.9647 (33)	6.30 (.30)	0.222 (.010)
.9444 (12) A	4.94 (.14)	.9866 (05)	.9886 (06)	.9882 (05)	.9639 (09)	6.51 (.12)	0.235 (.004)
.9376 (11) A	5.65 (.12)	.9837 (07)	.9882 (07)	.9905 (06)	.9628 (11)	6.86 (.13)	0.255 (.005)
.9027 (10) N	6.18 (08)	.9834 (18)	.9855 (13)	.9833 (16)	.9529 (29)	6.38 (.20)	0.300 (.010)

* Standard deviation x 10^4 in parentheses
\+ Standard deviation in parentheses

TABLE I. THE COMPRESSION OF FORSTERITE

V/V_o *	P +	a/a_o *	b/b_o *	c/c_o *	V/V_o *	U_{st} +	U_{pt} +
N: NaF A: Al	(GPa)	forsterite					
.9663 (02) N	1.75 (.01)	.9946 (08)	.9957 (03)	.9956 (02)	.9860 (09)	6.21 (.20)	0.087 (.003)
.9609 (04) A	3.30 (.04)	.9939 (06)	.9905 (03)	.9911 (03)	.9758 (08)	6.49 (.11)	0.157 (.003)
.9370 (02) N	3.59 (.02)	.9918 (14)	.9894 (05)	.9904 (04)	.9719 (15)	6.28 (.17)	0.177 (.005)
.9211 (17) N	4.73 (14)	.9901 (12)	.9853 (04)	.9883 (03)	.9641 (13)	6.38 (.15)	0.229 (.005)
.9280 (19) N	4.75 (.15)	.9905 (17)	.9863 (06)	.9877 (05)	.9650 (18)	6.43 (.19)	0.227 (.007)
.9394 (01) A	5.46 (.01)	.9908 (05)	.9849 (03)	.9861 (04)	.9623 (07)	6.69 (.07)	0.252 (.002)
.9072 (19) N	5.82 (.17)	.9901 (08)	.9819 (03)	.9853 (02)	.9579 (08)	6.54 (.12)	0.275 (.005)
.9004 (02) N	6.37 (.01)	.9884 (11)	.9816 (04)	.9836 (03)	.9542 (11)	6.56 (.08)	0.300 (.004)
.8998 (02) N	6.42 (.01)	.9897 (17)	.9808 (06)	.9837 (04)	.9549 (18)	6.63 (.14)	0.299 (.006)
.8825 (15) N	7.98 (.14)	.9844 (14)	.9777 (05)	.9819 (04)	.9450 (15)	6.70 (.11)	0.368 (.006)
.9164 (12) A	8.09 (.13)	.9826 (11)	.9766 (04)	.9808 (03)	.9412 (12)	6.52 (.08)	0.383 (.005)
.9108 (05) A	8.78 (.07)	.9848 (13)	.9762 (07)	.9800 (06)	.9421 (16)	6.85 (.10)	0.396 (.006)
.9021 (01) A	9.91 (.02)	.9829 (07)	.9726 (05)	.9784 (04)	.9354 (09)	6.88 (.05)	0.445 (.003)

* Standard deviation x 10^4 in parentheses
\+ Standard deviation in parentheses

BIBLIOGRAPHY

Ahrens, T. J. and E. S. Gaffney, Dynamic compression of enstatite, J. Geophys. Res., 76, 5504-5513, 1971.

Ahrens, T. J., J. H. Lower, and P. L. Lagus, Equation of state of forsterite, J. Geophys. Res., 76, 518-528, 1971.

Graham, E. K., Jr., and G. R. Barsch, Elastic constants of single-crystal forsterite as a function of temperature and pressure, J. Geophys. Res., 74, 5949-5960, 1969.

Frisillo, A. L. and G. R. Barsch, Measurement of single-crystal elastic constants of bronzite as a function of pressure and temperature, J. Geophys. Res., 77, 6360-6384, 1972.

Halleck, P. M. and B. Olinger, A method for the accurate measurement of lattice compressions of low-Z materials at pressures up to 12 GPa by x-ray diffraction, Rev. Sci. Instrum., 45, 1408-1410, 1974.

Kumazawa, M., The elastic constants of single-crystal orthopyroxene, J. Geophys. Res., 5973-5980, 1969.

Kumazawa, M. and O. L. Anderson, Elastic moduli, pressure derivatives and temperature derivatives of single-crystal olivine and single-crystal forsterite, J. Geophys. Res., 74, 5961-5972, 1969.

McQueen, R. G., S. P. Marsh, and J. N. Fritz, Hugoniot equation of state of twelve rocks, J. Geophys. Res., 72, 4999-5036, 1967.

Olinger, B. and P. M. Halleck, Compression and bonding of ice VII and an empirical linear expression for the isothermal compression of solids, J. Chem. Phys., 62, 94-99, 1975.

Olinger, B. and P. M. Halleck, The compression of α-quartz, J. Geophys. Res., in press, 1976.

Piermarini, G. J., S. Block, and J. D. Barnett, Hydrostatic limits in liquids and solids to 100 kbar, J. Appl. Phys., 44, 5377-5382, 1973.

Reid, A. M. and A. J. Cohen, Some characteristics of enstatite from enstatite achondrites, Geochim. Cosimochim. Acta, 31, 661-672, 1967.

Swanson, H. E. and E. Tatge, Standard X-ray Diffraction Powder Patterns, 1, p. 11 and p. 63, (NBS Cir. 539, U. S. Govern. Print. Off., 1953).

Fig. 1. The relative cell edges and volumes of forsterite at pressures to 10 GPa from the present work are shown as symbols. The ambient cell edge values are listed in the figure. The same relative values calculated by Graham and Barsch [1969] from ultrasonic data are shown as solid curves.

Fig. 2. The volume compression data for forsterite in the shock-particle velocity plane. The x-ray volume compression data are shown as the points with error bars on the left side of the figure; the solid line is a linear least squares fit to the data. The data of Ahrens, Lower, and Lagus [1971] are the points with error bars on the right side. The Hugoniots calculated from the ultrasonic work of Graham and Barsch [1969] and Kumazawa and Anderson [1969] are labeled "G & B" and "K & A".

Fig. 3. The relative cell edge and volumes of enstatite at pressures to 10 GPa from the present work are shown as symbols. The ambient cell edge values are listed in the bottom left portion of the figure. The same relative values calculated by Frisillo and Barsch [197]] from ultrasonic data for bronzite $(Mg_{.8},Fe_{.2})\ SiO_3$ are shown as solid curves. The ambient cell edge values for the bronzite are listed in the middle left portion of the figure.

Fig. 4. The volume compression data for enstatite in the shock-particle velocity plane. The x-ray volume compression data are shown as the points with error bars on the left side of the figure; the

solid line is an average linear fit with a forced slope of 5. The data of Ahrens and Gaffney [1971] are the points with error bars on the right side. The Hugoniot calculated from the ultrasonic work of Frisillo and Barsch [1972] for bronzite is labeled "F & B". The Hugoniot having the bulk sound speed as an intercept and an average slope to the shock data of Ahrens and Gaffney [1971] is shown as a broken line.

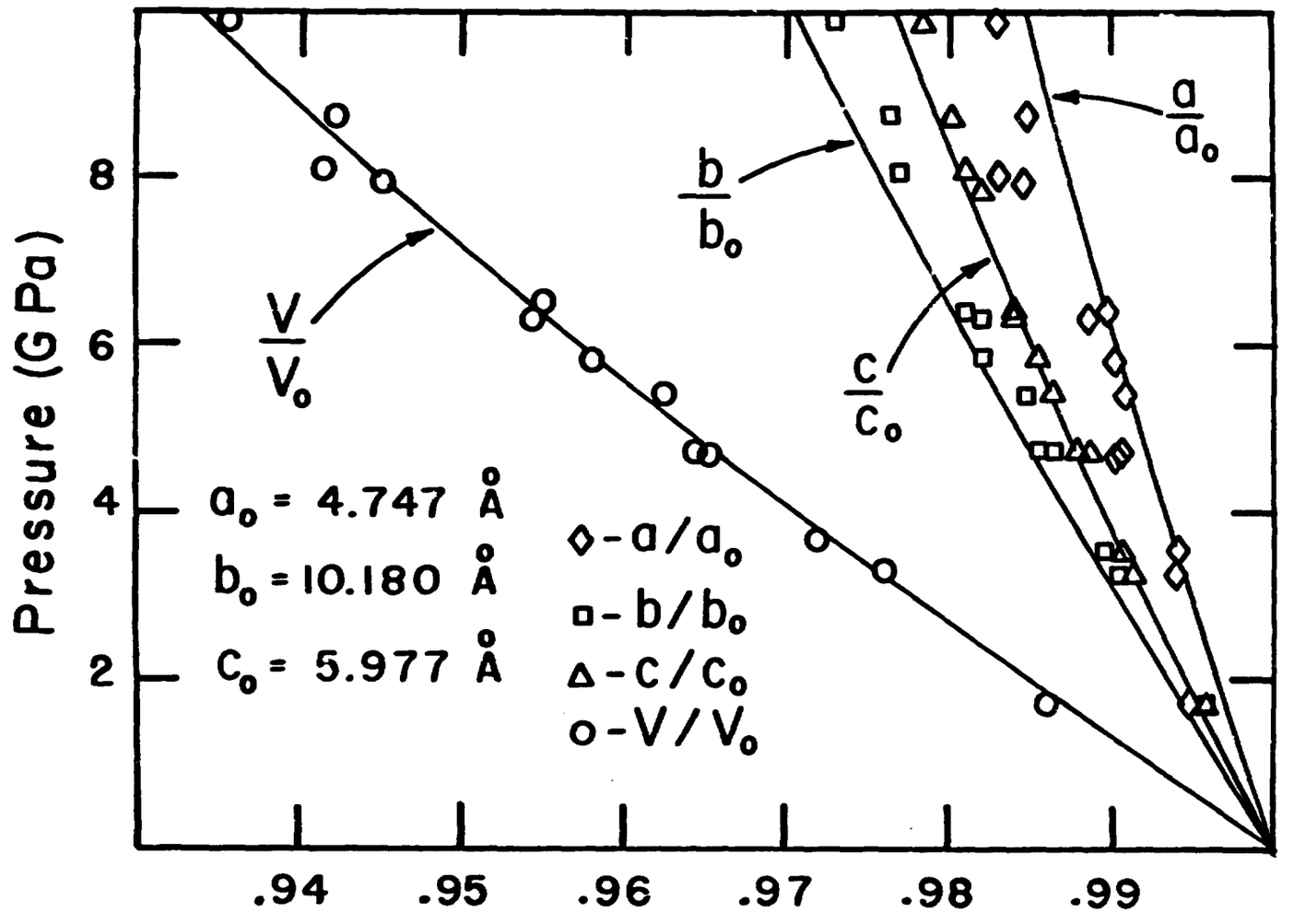
Pressure (G Pa)
8
6
4
2
.94
.95
.96
.97
.98
.99
V/V0
b/b0
a/a0
c/c0
a0 = 4.747 Å
b0 = 10.180 Å
c0 = 5.977 Å
◇ - a/a0
□ - b/b0
△ - c/c0
○ - V/V0

Figure 1

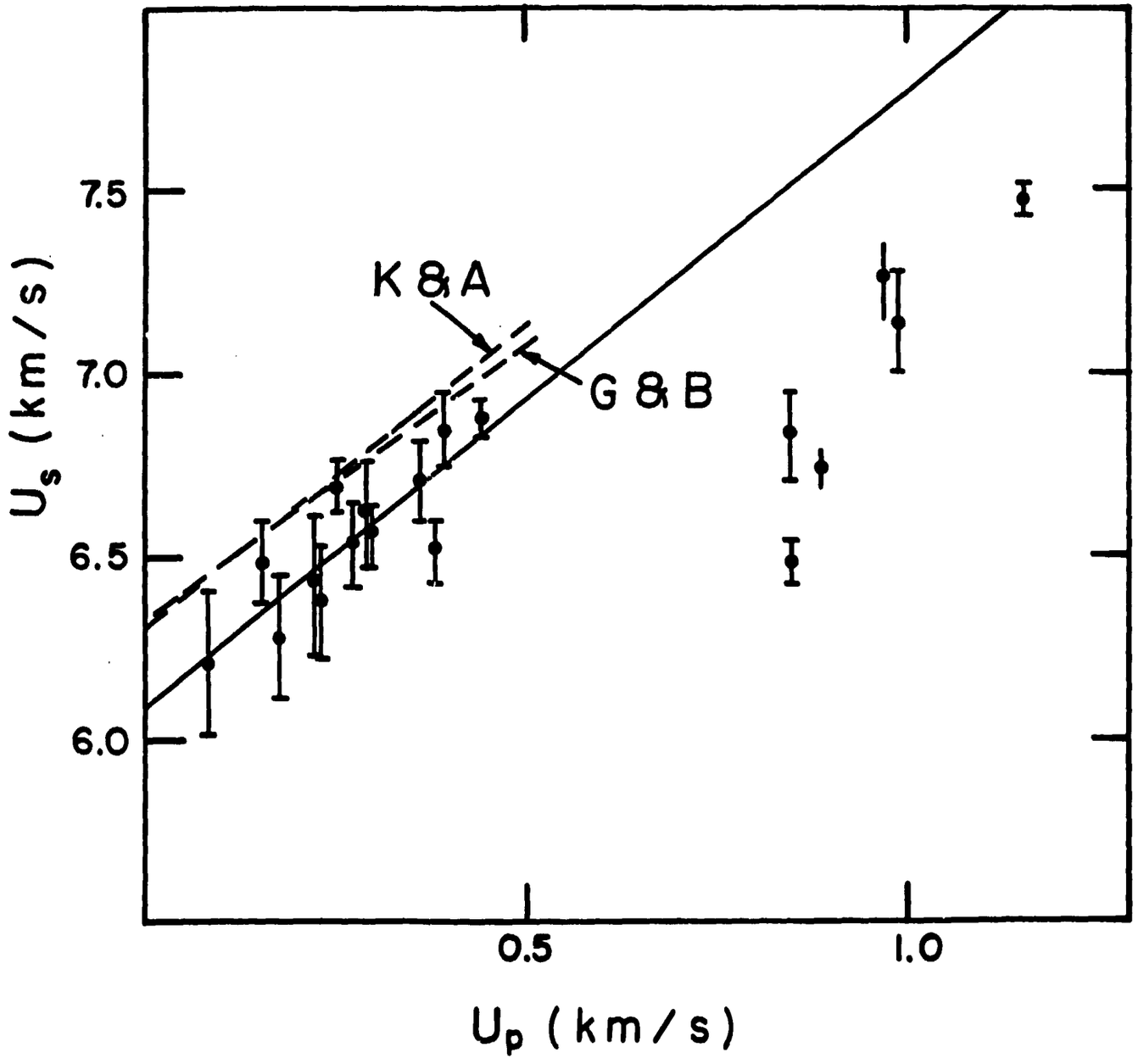

Figure 2

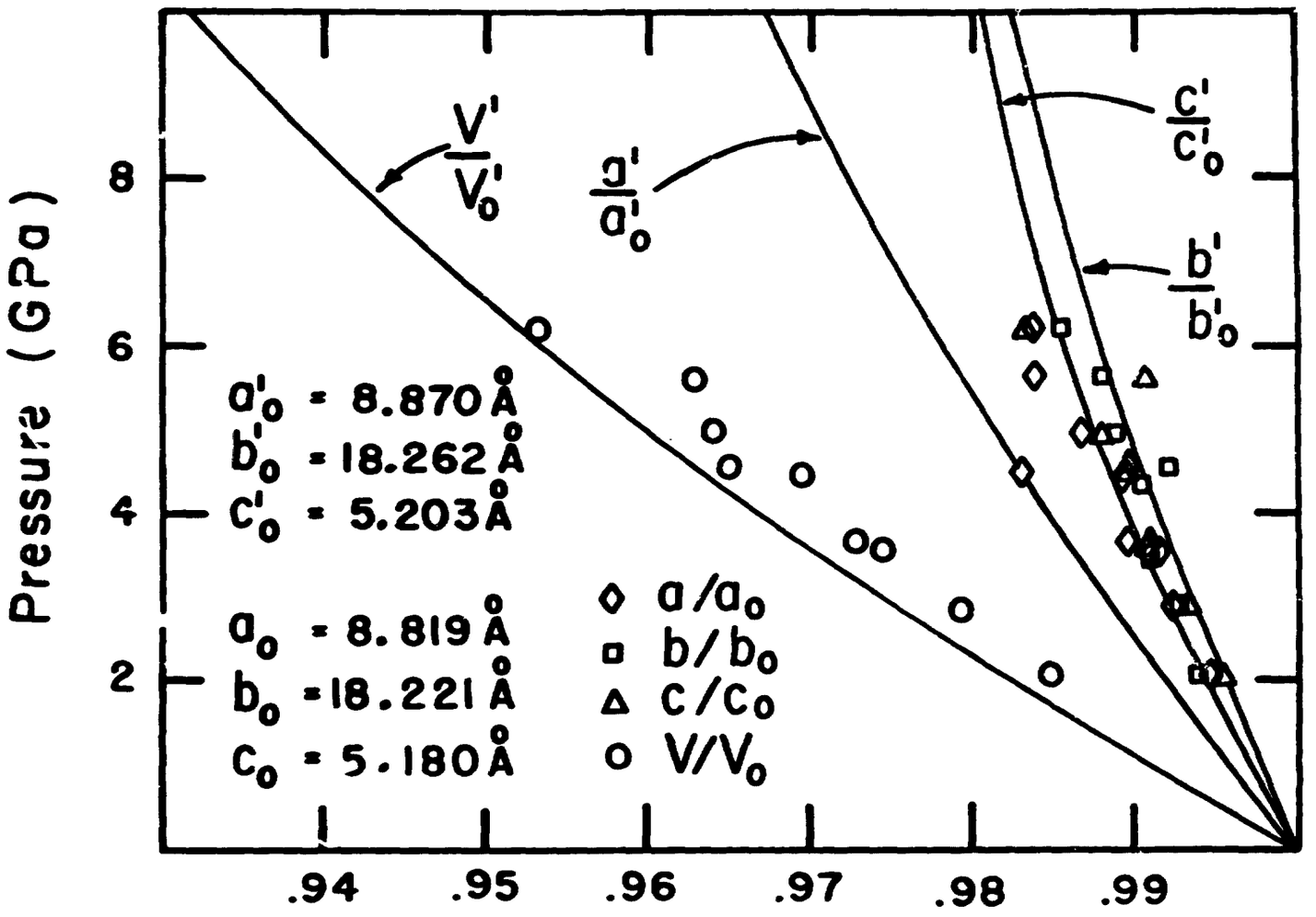
Pressure (GPa)
8
6
4
2
.94
.95
.96
.97
.98
.99
V'/V'0
a'/a'0
c'/c'0
b'/b'0
a'0 = 8.870 Å
b'0 = 18.262 Å
c'0 = 5.203 Å
a0 = 8.819 Å
b0 = 18.221 Å
c0 = 5.180 Å
◇ a/a0
□ b/b0
△ c/c0
○ V/V0

Figure 3

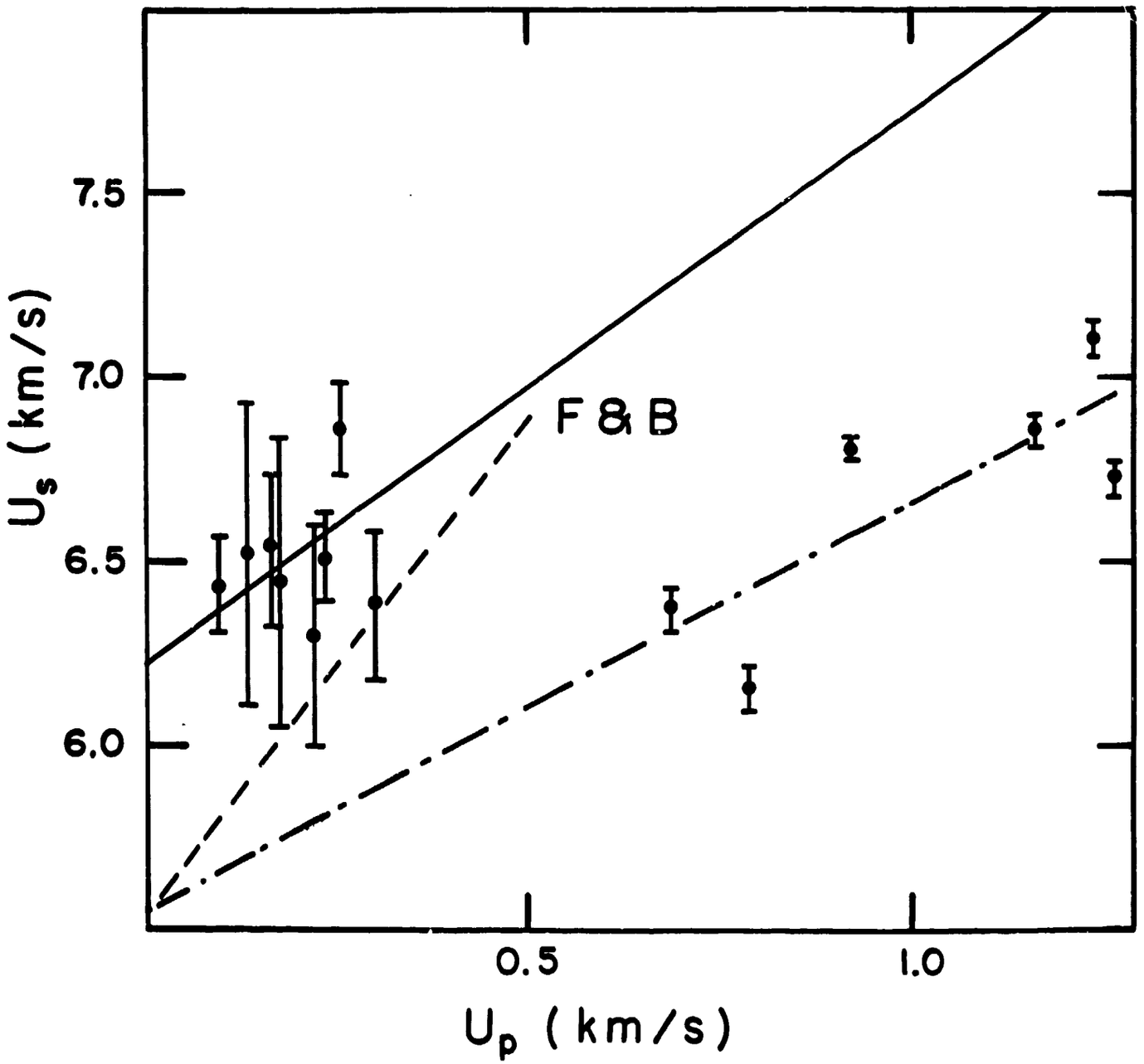

Figure 4